



Theoretical understanding of nova light curves

Physics and application

Mariko Kato

Dept. of Astronomy, Keio University, 4-1-1 Hiyoshi, Kouhoku-ku, Yokoyama, 223-8521,
Japan e-mail: mariko@educ.cc.keio.ac.jp

Abstract. I review current theoretical understanding of light curves of novae. Optical and infrared emissions are basically reproduced by free-free emission decaying as $t^{-1.75}$, independent of the white dwarf (WD) mass or chemical composition of the envelope. This property, we call it the universal decline law, is explained using the optically thick wind theory of nova outbursts. Using the universal decline law, we derive a theoretical relation between the maximum-magnitude and the rate of decline (MMRD). Theoretical light curves well reproduce observed data from low mass to very massive WDs close to the Chandrasekhar mass. Multiwavelength observation is required to determine the WD mass accurately because UV or soft X-ray light curves evolve with different parameter dependence. I also address some important issues related to light curve analysis, i.e., super-Eddington luminosity, no optically-thick wind evolution of PU Vul, transition from static to wind evolution in some slow novae, and helium nova.

Key words. binaries:close – binaries: symbiotic – novae, cataclysmic variables, Stars: mass loss – white dwarfs – X-rays:stars

1. Introduction

Novae are thermonuclear runaway events on a mass-accreting white dwarf (WD) in a close binary system. After the thermonuclear runaway sets in, the photosphere of the WD expands greatly up to $\sim 100 R_{\odot}$ or more, and the companion star is engulfed deep inside the photosphere. After the maximum expansion, the photospheric radius shrinks with time and free-free emission of expanding ejecta outside the photosphere dominates the optical and infrared emission. Due to strong wind mass-loss a large part of the envelope matter is blown in the wind and the photosphere moves inside. As the pho-

spheric temperature rises with time, the main emitting wavelength of photon shifts from optical to UV and then to supersoft X-rays. The optically thick winds continue until the photospheric temperature reaches $\log T$ (K) > 5.2 . The WD photosphere emits supersoft X-rays until hydrogen nuclear burning stops. Then the nova enters a cooling phase and finally the WD becomes dark. These timescales depends mainly on the WD mass and secondary on the chemical composition of the envelope. Therefore, multiwavelength observation is important to determine nova parameters.

The optically thick winds is accelerated due to a prominent peak of OPAL opacity at $\log T$ (K)=5.2, that locates deep inside the

Send offprint requests to: M. Kato

photosphere. Thus, the wind is a so called continuum-radiation-driven wind. The mass-loss rate is much larger than that of optically thin winds, namely, line-driven wind, which is accelerated outside the photosphere.

2. Nova light curve

2.1. A universal decline law

The decay phases of novae can be followed by a sequence of steady-state solutions. We solve the equations of motion, mass continuity, radiative diffusion, and conservation of energy, from the bottom of the hydrogen-rich envelope through the photosphere assuming steady-state. Evolutions of nova outbursts can be followed by a sequence of such steady-state solutions (Kato & Hachisu 1994).

Optical and infrared light curves are calculated assuming free-free emission which originates from the optically thin ejecta outside the photosphere. The free-free emission of optically thin ejecta is estimated by

$$F_\lambda \propto \int N_e N_i dV \propto \int_{R_{\text{ph}}}^{\infty} \frac{\dot{M}_{\text{wind}}^2}{v_{\text{wind}}^2 r^4} r^2 dr \propto \frac{\dot{M}_{\text{wind}}^2}{v_{\text{ph}}^2 R_{\text{ph}}}, \quad (1)$$

during the optically thick wind phase, where F_λ is the flux at the wavelength λ , N_e and N_i are the number densities of electrons and ions, respectively, R_{ph} is the photospheric radius, \dot{M}_{wind} is the wind mass-loss rate, v_{ph} is the photospheric velocity, and $N_e \propto \rho_{\text{wind}}$ and $N_i \propto \rho_{\text{wind}}$. These \dot{M}_{wind} , R_{ph} , and v_{ph} are calculated from our optically thick wind solutions. As the wind mass-loss rate quickly decreases with time the flux at a given wavelength also decreases with time. Note that the shape of the light curve is independent of the wavelength, whereas the absolute magnitude, i.e., proportionality constant of Equation (1) depends on it. This wavelength-free light curve is one of the characteristic properties of free-free emission (see Hachisu & Kato 2006).

Figure 1 shows calculated light curves for various WD masses. The light curve decays quickly in more massive WDs, mainly because of smaller envelope masses. Observational y magnitudes of V1668 Cyg follows very well our $0.9 M_\odot$ WD model.

If we plot these light curves in a logarithmic time since the outburst, the light curve decays as $t^{-1.75}$ independently of the WD mass except the early phase near the peak and a later phase where emission lines dominate. If we further multiply by a

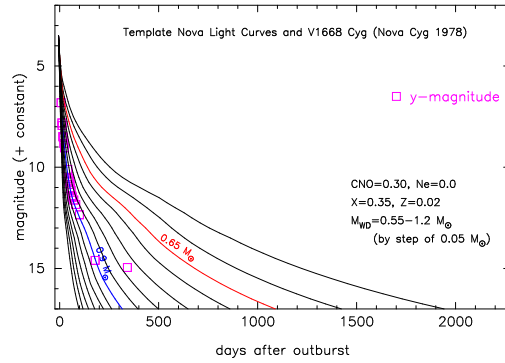


Fig. 1. Our model free-free light curves for various white dwarf masses, from 0.55 to $1.2 M_\odot$ for optical and infrared band. The decay timescale depends mainly on the white dwarf mass. Observational y magnitudes of V1668 Cyg (1978) (open squares: Gallagher et al. 1980) are well fitted to $0.9 M_\odot$ WD model (taken from Hachisu & Kato 2010).

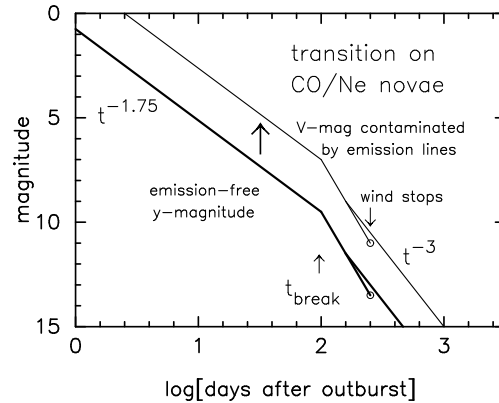


Fig. 2. Schematic nova light curve for free-free emission model. Nova light curve decays as $t^{-1.75}$. When the nova enters the nebular phase and strong emission lines dominate, the light curve is lift up (thin solid line) from the template nova light curve (thick solid line).

some factor, i.e., shift in the horizontal direction in logarithmic timescale, all the light curves essentially converge into a single curve (for the factor see Tables 2 and 3 in Hachisu & Kato 2010). This template light curve is plotted in Figure 2. After the peak magnitude, the main body of a optical/infrared light curve decays as $t^{-1.75}$ (thick line) until the nova enters the nebular phase. When strong emission lines, such as [O III], begin to contribute to the optical flux, the light curve is gradually lift up from the

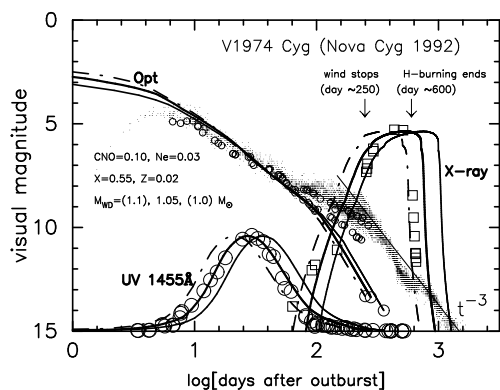


Fig. 3. Light curve fitting of V1974 Cyg. Calculated optical, UV and X-ray fluxes from the WD photosphere are plotted against time for WD masses of 1.0 (right), 1.05 and 1.1 M_{\odot} (left). The large open circles at the right end of optical light-curve denote the epoch when the optically thick wind stops. Dots and open circles represent visual and V magnitude, respectively. There is a systematic discrepancy in V -magnitudes among different V systems due to contamination of emission lines at the shorter edge of the V -bandpass. The difference becomes more prominent in the later nebular phase. Large circles represent IUE data, and squares supersonic X-ray data (taken from Hachisu & Kato 2006)

template nova light curve and decays as the thin line. When the optically-thick winds stops, the magnitude decays as t^{-3} . We recommend observations with narrower band filters such as Strömgren y -band to accurately follow continuum flux even in the nebular phase (taken from Hachisu & Kato 2006).

2.2. MMRD relation

There is a well known empirical relation between the maximum absolute magnitude and the rate of decline (MMRD) of nova light curves (e.g. Schmidt 1957). A brighter nova decays more rapidly. Using the universal decline law, we can derive a theoretical MMRD relation. If we take a typical maximum magnitude for a WD, we get a decline rate from the template light curve (Figure 2). This template curve is common for all the WD mass with some squeeze/expand factor of the timescale and the magnitude. Therefore, for a arbitrarily chosen WD mass, we get the maximum value of the light curve and corresponding decline rates. In this way Hachisu & Kato (2010) derived a theoretical MMRD re-

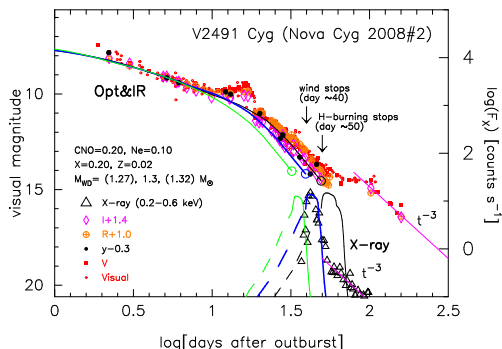


Fig. 4. Light curve fitting of V2491 Cyg. Theoretical free-free and supersoft X-ray light curves are depicted by the solid lines: from left to right, 1.32 M_{\odot} (green line), 1.3 M_{\odot} (thick blue line), and 1.27 M_{\odot} (thin black line). The best-fit model, that reproduce the optical and X-ray light curves simultaneously, is 1.3 M_{\odot} WD with the envelope chemical composition of $X = 0.20$, $Y = 0.48$, $X_{\text{CNO}} = 0.20$, $X_{\text{Ne}} = 0.10$, and $Z = 0.02$. *Large open triangles*: observational X-ray (0.2–0.6 keV) count rates obtained with *Swift*. The $F_{\lambda} \propto t^{-3}$ law (magenta) is added for the nebular phase (taken from Hachisu & Kato 2009)

lation which is very consistent with observationally derived empirical relations. It is well known that MMRD relation stands for only an average and is not so accurate for individual nova. This properties is naturally explained as an intrinsic deviation due to a different ignition mass associated with a different mass-accretion rate. (see Fig. 15 and Section 5 in Hachisu & Kato (2010) for more detail.)

2.3. Light curve fitting for V1974 Cyg and V2491 Cyg

Figure 3 shows light curve fitting of V1974 Cyg. The optical light curve decays as $t^{-1.75}$ from the optical peak at $t = 2.67$ days until the strong emission lines begin to contribute in the nebular phase. This figure also shows UV 1455 Å narrow band light curve. This bands is selected to avoid prominent emission or absorption lines in UV spectra and to represent continuum emission (Cassatella et al. 2002). Changing the WD mass for a given chemical composition of the envelope, one can choose a best fit model that reproduces the light curves of optical, UV and supersoft X-ray simultaneously, which is shown in the figure.

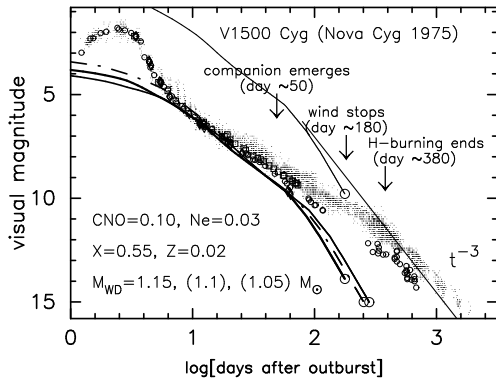


Fig. 5. Light curve fitting of V1500 Cyg. Dots represent visual and *V*-band observations and small open circles *y*-magnitudes. Theoretical free-free emission light curve are plotted for three WD masses of 1.1, 1.15 and 1.2 M_{\odot} (taken from Hachisu & Kato 2006).

Another example of light curve fitting is given in Figure 4. V2491 Cyg is a classical nova that shows the second maximum at $t \sim 16$ day. The light curve follows the universal decline law except the second peak which is explained as a magnetic activity (Hachisu & Kato 2009). The decline is very fast and supersoft X-ray phase lasts only 10 days. Hachisu & Kato (2009) presented light curve model of 1.3 M_{\odot} WD. Note that the decay light curve is almost identical in *y*, *R*, and *I* bands, which is a characteristic property of free-free emission.

3. super-Eddington luminosity

The super-Eddington luminosity is one of the long standing problems in theoretical study of classical novae. Super-Eddington phases last several days or more around the optical maximum, and the peak luminosities often exceed the Eddington limit by a factor of a few to several. It is difficult to reproduce such a super-Eddington luminosity in dynamical calculations of nova outbursts, probably because of numerical difficulty or adopted assumptions.

3.1. Porous instability

Shaviv (2001) presented an idea of reduced opacity in a porous envelope for the mechanism of super-Eddington luminosity (see Shaviv's proceedings of this conference). Based on his idea, Kato & Hachisu (2007) calculated trial light curve models that reproduce optical light curves in the super-Eddington

phase as well as *IUE* UV light curves in the post-super Eddington phase for five classical novae. The duration and the excess of super-Eddington luminosities are, for example, (0.84 mag, 6 days) for V693 CrA, (1.7 mag, ~ 17 days) for V1974 Cyg, (~ 1.8 mag, 16 days) for V1668 Cyg, i.e., the super-Eddington phase is relatively short in the total duration of nova outbursts. However, porous instability has not yet been studied in a realistic nova envelope. Thus, for example, we don't know why there is no super-Eddington phase in some novae, e.g., like slow nova PU Vul (see Section 4). In this sense, the idea of porous instability has not yet fully established.

3.2. "Normal" super-Eddington novae vs. "super-bright" novae

della Valle (1991) proposed 'super-bright' novae, as a subgroup of classical novae in which the peak magnitude is ~ 1 mag brighter than the prediction of the MMRD relation. Several novae, e.g. LMC 1991 and V1500 Cyg, show a very bright peak, thus belong to the super-bright nova, whereas majority of novae follow the MMRD relation with a certain range of scatters.

In a theoretical side, the universal decline law (Figure 2) has explained a large number of nova light curves (e.g. Hachisu & Kato 2007). This theoretical light curve naturally extends beyond the Eddington luminosity. For example, V1974 Cyg (Figure 3) decays along with the universal decline law, in which the first 17 days is the super-Eddington phase.

Hachisu & Kato (2007) pointed out that the majority of novae follow the universal decline law, like V1974 Cyg. I may call them 'normal super-Eddington novae', whereas superbright novae show a 1.5–2 mag brighter peak than the universal decline law. For example, Figure 5 shows the light curve of V1500 Cyg in which the peak magnitude is about 2 mag brighter than the universal decline law. V1500 Cyg is a very bright fast nova and is well observed in multiwavelength bands. In the super-bright phase V1500 Cyg showed blackbody spectra, which gradually changed to that of free-free (Gallagher & Ney 1976). This suggests that the emission mechanism in the super-bright phase is different from that of the "normal" super-Eddington luminosity.

Therefore, we may have a tentative theoretical definition of super-bright nova as a nova with peak magnitude brighter than the prediction of universal decline law. As shown in Section 2.2, a MMRD relation is derived from the universal decline law,

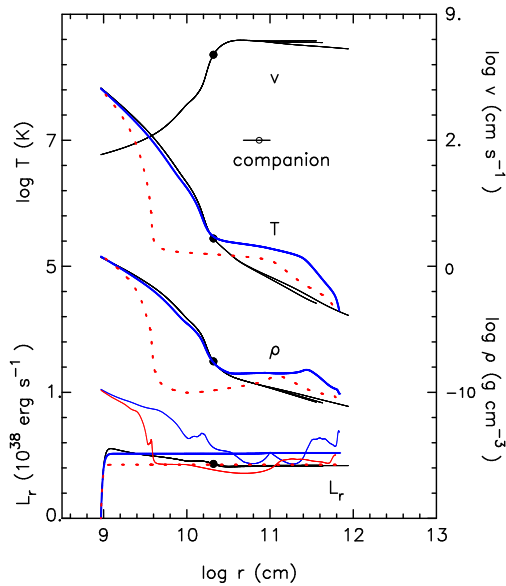


Fig. 6. Comparison of the static and optically thick wind solutions of a $0.55 M_{\odot}$ WD with a $0.4 M_{\odot}$ MS companion. The left/right edge of each line corresponds to the bottom/photosphere of the envelope. Dotted lines represent the static solution without effects of companion and thick lines the static solution in which the companion effect is taken into account. The Eddington luminosity (Equation (2)) is plotted by the thin solid line (lower/upper) for the static solution with/without companion effects. Optically thick wind solutions are depicted by the thin solid lines with a dot that indicates the critical point. The location of the companion and the size of accretion radius are indicated by the small open circle with a short horizontal bar. (made from Kato & Hachisu 2011)

this definition is consistent with that given by della Valle. The super-bright novae are relatively rare, but the list includes V1500 Cyg (Figure 5), V597 Pup (2007) (for the light curve, see Fig. 20 in Hachisu & Kato 2010), GQ Mus (Fig. 7 in Hachisu et al. 2008), V1493 Aql (Fig. 3 in Hachisu & Kato 2009).

4. No optically thick winds – PU Vul

Kato & Hachisu (2009) showed that the optically thick winds occur in massive WDs ($\geq 0.7 M_{\odot}$), but do not occur in less massive WDs ($\leq 0.5 M_{\odot}$: the boundary depends on the chemical composition), whereas in the intermediate WD mass region ($\sim 0.5 - 0.7 M_{\odot}$) both types of solution are realized. When

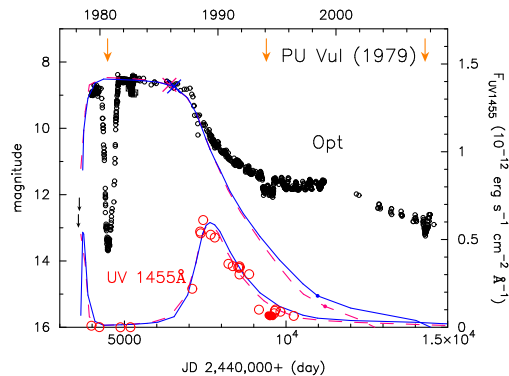


Fig. 7. Optical and UV light curves of PU Vul. Large open circles denote the continuum flux of *IUE* UV 1455 Å band. The scale in the right-hand-side denotes that for observational data. No optically thick wind occurs. Solid and dashed lines denote theoretical nova model of 0.57 and $0.6 M_{\odot}$ WD. The downward arrow indicates the epoch of eclipse. Taken from Kato et al. (2011).

the optically thick wind does not occur, we solve equation of hydrostatic balance instead of equation of motion. In this case the structure of the envelope is very different from that of the wind solution. Figure 6 shows distribution of the temperature, density, diffusive luminosity, and the local Eddington luminosity, which is defined as

$$L_{\text{Edd}} \equiv \frac{4\pi c G M_{\text{WD}}}{\kappa}, \quad (2)$$

where κ is the OPAL opacity. Since the opacity κ is a function of the temperature and density, the Eddington luminosity is also a local variable. This Eddington luminosity has a local minimum at $\log T$ (K) = 5.25 corresponding to the opacity peak.

This figure also shows internal structures of optically thick winds. These two kind of envelopes are very different in the density and temperature distributions. The optically thick wind envelope (thin line with a black dot) shows monotonic decrease in the density distribution (as r^{-2} at $\log r$ (cm) ≥ 10.3), while the static solution develops a large density-inversion region at $\log r$ (cm) $\sim 9.6 - 11$. This density-inversion arises in order to keep hydrostatic balance in the super-Eddington region ($L_{\text{Edd}} < L_r$) as expected from the equation of hydrostatic balance.

In symbiotic nova, PU Vul, which showed no indication of strong wind mass-loss in its spectrum during the flat peak. Figure 7 shows the theoretical models calculated by Kato et al. (2011). As no optically thick winds occur, the evolution timescale is

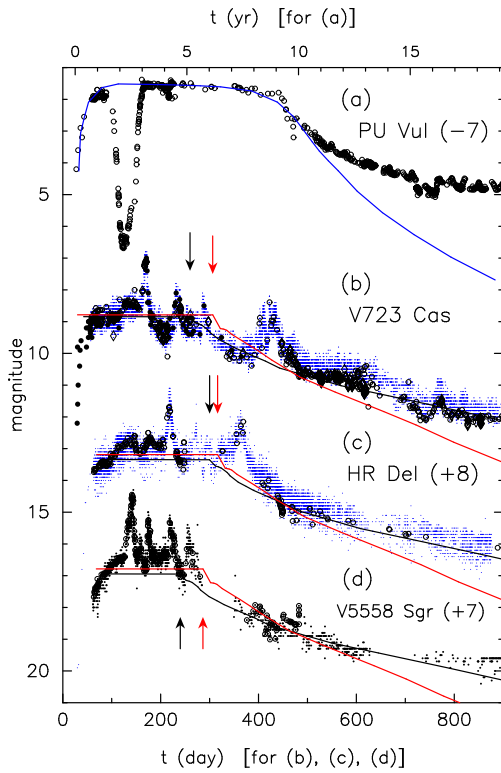


Fig. 8. Light curves of four slow novae. The upper timescale is for PU Vul and lower one is for the other three novae. (a) PU Vul: The dips at $t = 2.2$ yr and 15.7 yr are eclipses. (b) V723 Cas. (c) HR Del. (d) V5558 Sgr. The solid lines indicate the composite light curve model of $0.55 M_{\odot}$ WD with $X = 0.55$, $C + O = 0.2$, $Z = 0.02$ (red line), and $0.6 M_{\odot}$ WD with the solar composition (black line). The arrows indicate the switching point from a static to a wind evolution.

as long as a decade, thus the envelope keeps low surface temperatures several years. This is the reason why PU Vul shows a long-lasting flat optical maximum. This makes a remarkable contrast with a majority of novae that shows a sharp peak because strong optically thick winds blow off a large part of the envelope in a very short timescale. As no optically thick winds occurs, PU Vul does not follow the universal decline law, nor MMRD relation.

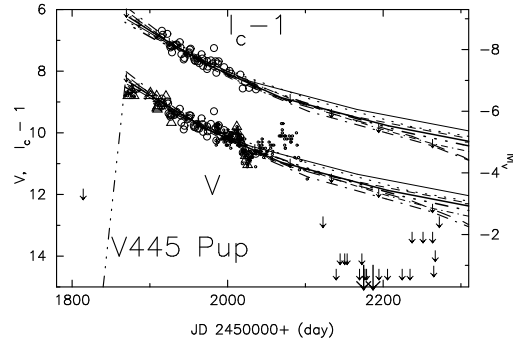


Fig. 9. Light curve fitting of the helium nova V445 Pup. Lines indicate theoretical models for 1.35 , 1.37 and $1.377 M_{\odot}$ WD. See Kato et al. (2008) for detail.

5. Transition nova – from static to wind evolution

PU Vul is a long orbital period binary ($P_{\text{orb}} = 13.4$ yr, whereas classical novae are close binaries. If the companion is close enough it is engulfed by the extended envelope of the WD during the nova outburst. Kato & Hachisu (1994) confirmed that the nova envelopes are not much affected by the presence of the companion (see their Figure 6 also Section 5) as far as the optically thick winds blow. However, the static envelope is largely affected by the companion's gravity.

Figure 6 compares the envelope models with (blue lines) and without (red dotted lines) companion effects. In the envelope with companion effects, the envelope matter is significantly re-distributed due to the companion's effects. With the companion's gravity, the Eddington luminosity, outside the orbit, $L_{\text{Edd}} = 4\pi c G(M_{\text{WD}} + M_{\text{comp}})/\kappa$, is larger than that without companion $L_{\text{Edd}} = 4\pi c G M_{\text{WD}}/\kappa$. This difference causes a different energy flux, which makes the two envelopes in different hydrostatic balance. A lower luminosity leads to a larger local-super Eddington region which causes a wider density-inversion region.

Some classical novae shows flat light curve with oscillatory behavior without indication of strong wind mass-loss, followed by a smooth decline with massive winds. Kato & Hachisu (2009) presented an idea of transition from static to wind solution during a nova outburst. Kato et al. (2011) calculated light curves for such a 'transition nova' as shown in Figure 8. These novae show oscillatory behaviors in the flat phase which may correspond to a relaxation process associated with the transition from static to wind solutions.

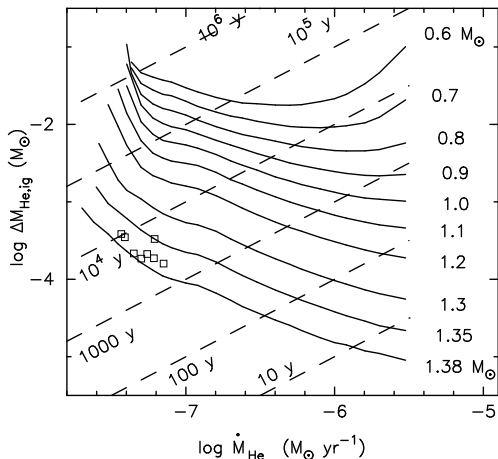


Fig. 10. The helium ignition mass, $\Delta M_{\text{He,ig}}$, of helium-accreting WDs is plotted against the helium accretion rate, \dot{M}_{He} . The WD mass is attached to each curve. Straight dashed lines indicates the recurrence period. The open square indicates the ignition mass of models in Kato et al. (2008).

6. Helium nova – V445 Pup

Helium novae are similar phenomena to ordinary novae, but nuclear fuel is helium. If the companion star is a helium star, the WD accretes helium until the accreted matter reaches a critical value, thus unstable helium burning triggers a thermonuclear runaway event. If the companion is a normal star, and the hydrogen accreting WD is growing in mass (like recurrent novae or SSS), a helium ash layer develops underneath the hydrogen burning zone, which also triggers a helium nova outburst. Such helium novae were theoretically predicted by Kato et al. (1989) long before V445 Pup was discovered in 2000 December, which is the only helium nova detected so far.

Fig. 9 shows the light curve of V445 Pup, which show a slow decline in V and I bands before the blackout due to dust formation. We have only 210 days data available for light curve analysis. As V and I magnitude decays almost parallel, which is the characteristic properties of free-free emission, we can apply the universal decline law also to this helium nova. From the light curve fitting the WD mass is estimated to be very massive ($\geq 1.35 M_{\odot}$) and the WD is growing in mass with a high efficiency (see Kato et al. (2008) for more detail). Therefore, V445 Pup is a candidate of SN Ia progenitors.

Fig. 10 shows the relation between the ignition mass and helium accretion rate. A helium deto-

nation occurs in low accretion rates ($\log \dot{M}_{\text{He}} (M_{\odot} \text{ yr}^{-1}) < -7.6$) which may cause a kind of subluminous supernova explosion rather than normal SNe Ia. If the WD accretes hydrogen in a steady state, i.e., in the wind phase or supersoft X-ray phase of SN Ia progenitor models, the helium accretion rate is about -6.0 – $-6.3 M_{\odot} \text{ yr}^{-1}$ for $\geq 1.3 M_{\odot}$ WDs, and most of the accreted matter accumulates on the WDs because helium shell flash is very weak. V445 Pup correspond to $\log \dot{M}_{\text{He}} (M_{\odot} \text{ yr}^{-1}) = -7.2$ – -7.4 ; The model envelope mass, obtained from the light curve fitting, is plotted by the open squares. The companion star of V445 Pup is an evolved helium star, and is filling its Roche lobe and transferring its mass by the rate above. However, its binary evolutionary path is not known.

7. Discussion

NIR SHAVIV: You have shown an explanation to the oscillation in slow novae, that it switches between to solutions with a wind and without, and that it is due to a change gravitational potential by the companion. Should you expect to see variations with the orbital frequency.

MARIKO KATO: It is very interesting if there found a dependence between the oscillatory behavior and the orbital period. However, the the quasi oscillation period may depends on the WD mass and companion mass as well as the orbital period. We may not able to separate each contributions, because we have only a few well-observed objects.

GIORA SHAVIV: How fast is the transition between the two solutions? What happen to the energy distribution between the two solutions?

MARIKO KATO: I think the transition occurs in several dynamical timescale of the outerpart of the envelope. The dynamical timescale is estimated to be $t_{\text{dyn}} \sim (2/GM)^{1/2} r^{3/2} = 21$ days for $r = 6 \times 10^{12}$ cm and $M = 0.95 M_{\odot}$. Here I assume the total mass of the binary (WD + companion) to be $0.95 M_{\odot}$. This timescale is roughly consistent with the magnitude variation of the novae in Figure 8. So I suppose these oscillatory magnitude variation may associate with a relaxation process. The static solution has a larger internal energy than the wind solution of the same mass, so the excess energy may be radiated during the transition process.

References

- Cassatella, A., Altamore, A., & González-Riestra, R. 2002, *A&A*, 384, 1023
della Valle, M. 1991, *A&A*, 252, 9

- Gallagher, J. S., & Ney, E. P. 1976, ApJ, 204, L35
Gallagher, J. S., Kaler, J. B., Olson, E. C., Hartkopf, W. I., & Hunter, D. A. 1980, PASP, 92, 46
Hachisu, I., & Kato, M. 2006, ApJS, 167, 59
Hachisu, I., & Kato, M. 2007, ApJ, 662, 552
Hachisu, I., & Kato, M. 2009, ApJ, 694, L103
Hachisu, I., & Kato, M. 2010, ApJ, 709, 680
Hachisu, I., Kato, M., & Cassatella, A. 2008, ApJ, 687, 1236
Kato, M., & Hachisu, I., 1994, ApJ, 437, 802
Kato, M., & Hachisu, I. 2004, ApJ, 613, L129
Kato, M., & Hachisu, I. 2007, ApJ, 657, 1004
Kato, M., & Hachisu, I. 2009, ApJ, 699, 1293
Kato, M., & Hachisu, I. 2011, ApJ, in press
Kato, M., Hachisu, I., & Cassatella, A., 2011, ApJ, 704, 1676
Kato, M., Hachisu, I., Cassatella, A., & González-Riestra R. 2011, ApJ, 727, 72
Kato, M., Hachisu, I., Kiyota, S. & Saio, H. 2008, ApJ, 684, 1366
Kato, M., Saio, H. & Hachisu, I. 1989, ApJ, 340, 500
Schmidt, Th. 1957, Z. Astrophys., 41, 181
Shaviv, N. J. 2001, MNRAS, 326, 126